CHAPTER 1

Introduction and Scope of the Thesis

1.1 Introduction

Industrial development, automation, and the fast-growing population have increased the global requirement for energy. The energy demands in economically emerging countries are estimated to be increased by 90% in 2035 [1]. Moreover, energy production (electricity) is still less than the current demand, and about 20% of the global population are facing electricity problem [1]. Presently, most of the electricity is produced by traditional fossil fuels, namely coal, oil, and gas. However, the decreasing natural stock of fossil fuels will affect future energy requirements. The generation of electrical energy from fossil fuels also creates severe environmental issues such as global warming through the greenhouse effect and air pollution by releasing carbon monoxide, sulphur dioxide, carbon dioxide, nitrogen dioxide, and other gases [2]. Therefore, the sustainable and green energy source is adopted nowadays to overcome the environmental issues and the shortage of fossil fuels. Renewable energy sources such as sun, wind, geothermal, hydroelectric, and biomass are examples of sustainable and green energy resources, as shown in Figure 1.1 [3]. The sun is one of the most important renewable energy sources among the various renewable energy resources due to the abundant sunlight availability. A photovoltaic device converts solar radiation (photon energy) into electrical energy similar to the natural photosynthetic process (convert solar radiation energy into another form of energy such as the chemical potential) in plants [4].

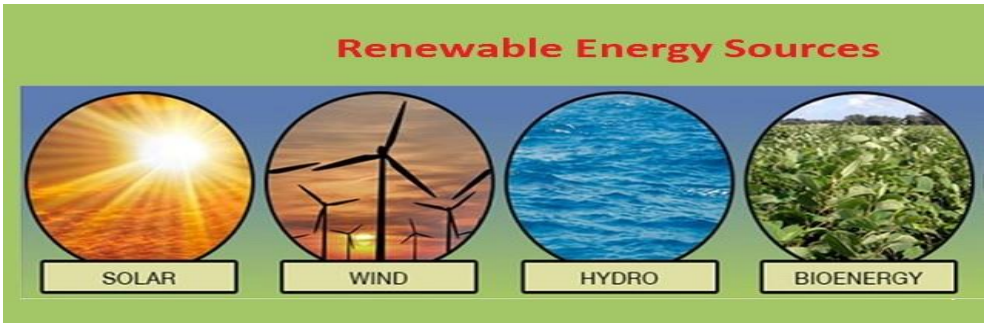

Figure 1.1: Renewable energy resources [3].

1.2 Photovoltaic Devices

The 'photovoltaic effect' is a phenomenon in which photon energy is converted into electrical energy (voltage and current). The photovoltaic effect was first observed by French physicist A. E. Becquerel in 1839 [5]. He found a generated voltage and current in his experiment when he placed silver chloride in an acidic solution and illuminated it with light. Initially, this effect was also known as the "Becquerel effect"[5]. In 1876, photoconductivity was found by William Adams and Richard Day in a thin layer of selenium when sandwiched between two heated platinum contacts [6]. In 1883 C.E. Fritts has given a new form of selenium cells which was extremely sensitive to light than any other cells discovered before. In 1914, Goldman and Brodsky observed that the photovoltaic effect is due to the existence of a barrier that drives the charge carrier in the opposite direction in the photodiode-like structures. The flow of charge carriers constitutes the photocurrent, and the conduction mechanism at semiconductor/semiconductor or semiconductor/metal interfaces was developed by Walter Schottky in 1941 [7].

On the other hand, the manufacturing of good quality silicon wafers in the 1950s gave rise to the development of solid-state electronics and efficient photovoltaic devices

[8]. Further, the realization of the positively (p) and negatively (n) doped silicon led to the manufacturing of silicon p-n junction structures, which have shown a much better-rectifying property than Schottky barriers and better photovoltaic behaviour. In 1954, Daryl Chapin, Calvin Fuller, and Gerald Pearson, scientists of Bell Laboratories, accidentally found while doing experiments with semiconductors that silicon doped with certain impurities was very sensitive to light [9]. They invented the first practical device for converting sunlight into useful electrical power, resulting in the production of the first practical solar cell with an efficiency of around 6% [9]. Later, the researchers have shown a lot of effort to improve the silicon solar cell's performance. Commercially, silicon is the most widely used material for the fabrication of solar cells, but the high fabrication cost of silicon-based devices (due to high-temperature processing) [10], high energy payback time (EPBT) (due to large energy requirement for converting silica into silicon) [11] and difficulties in managing the electronic waste resulted from silicon devices have led to a new area of research in organic solar cells (OSCs).

1.3 Organic Photovoltaic (OPV) Devices

Silicon photovoltaic technology currently dominates the commercial production of photovoltaic cells, but whenever cost and mechanical properties come into consideration over the performance and lifetime, organic photovoltaic technology comes into the picture. The beginning of the 20^{th} century or the end of the 19^{th} century was the era of organic devices. Organic devices opened the scope of OSC and developed the interest among the researchers to work in OSC at the commercial level. The organic materials have shown synthesis-dependent several favourable properties, such as bandgap tuning, electronic and optical properties enhancement, etc. The first

photo conducting phenomenon in the organic compound was observed in anthracene and analyzed by Pochettino in 1906 [12]. The first organic photovoltaic (OPV) device was fabricated by Tang in 1986 [13] with a power conversion efficiency of 1%. Recently, organic photovoltaic technology has shown a more considerable impact in the field of photovoltaic over inorganic photovoltaic technology. The charge carrier conduction mechanism in the organic materials is not identical to the inorganic materials. Therefore, the organic materials properties are briefed in the next subsection before discussing different types of organic solar cells and their working mechanisms.

1.3.1 Materials for Organic Photovoltaic Cells

The electronics structures of organic and inorganic semiconductors are entirely different from each other. In inorganic semiconductors, atoms are bonded with the covalent bond to form a crystalline structure where electrons are spatially delocalized over the crystalline lattice. These electrons are distributed over energy states that comprise the semiconductor valence band and conduction band. These bands are continuous energy bands separated by an energy gap, known as energy bandgap (Eg). In inorganic photovoltaic, electrons of the valence band are jumped into the conduction band upon light absorption, and these excited electrons in the conduction band are driven to the electrodes utilizing an electrical field.

On the other hand, organic semiconductors are conjugated molecular or polymeric compounds whose energy band gap is defined by the difference between the highest occupied molecular orbital (HOMO) to the lowest occupied molecular orbital (LUMO). Polyaniline was the first organic semiconductor, synthesized by the anodic oxidation of aniline in 1862 [14]. Carbon and hydrogen atoms are the basic building blocks for any

organic semiconductor, and also some other heteroatoms such as nitrogen, sulphur, oxygen, etc., are used depending upon electronics application. Conjugated polymers are those where alternating C-C bonds (σ-bonds) and C=C bonds (π-bonds) exist in the polymer chain, which makes them conducting in nature and used for the optoelectronic application [15]. The valence band (VB) theory describes the covalent bond between the atoms but has limitation that it can not describe the alternating double and single bonds associated with the conjugated polymers. Therfore, molecular orbital (MO) theory was developed to describe the covalent bonds in the conjugated polymers. According to the MO theory electrons are distributed in a set of molecular orbital and can be extended over entire molecule. MO theory includes the two different combination of molecular orbital, one is bonding orbital and another is anti bonding orbital. Bonding orbitals are formed by σ-orbital and π-orbital whereas, anti bonding orbitals are formed by σ*-orbital and π*-orbital as shown in Figure 1.2. The σ-orbital is completely filled and at the lowest energy level, whereas the σ*-orbital is empty and at the highest energy level. The strong net attractive interaction among the nuclei is due to the bonding and anti-bonding in σ-orbital that holds the molecule together. However, due to the less attractive interaction of π-bonds, splitting takes place to form π- and π*-orbitals. π-orbitals are filled whereas, π*-orbitals are empty. Similar to the valence band in the inorganic semiconductor, there is the highest occupied molecular orbital (HOMO) consisting of π-orbitals. On the other hand, like conduction band in an inorganic semiconductor, there is a lowest unoccupied molecular orbital (LUMO) consisting of π*-orbitals. The comparison of the simplified energy band diagram of a conjugated polymer and inorganic semiconductor is shown in Figure 1.2.

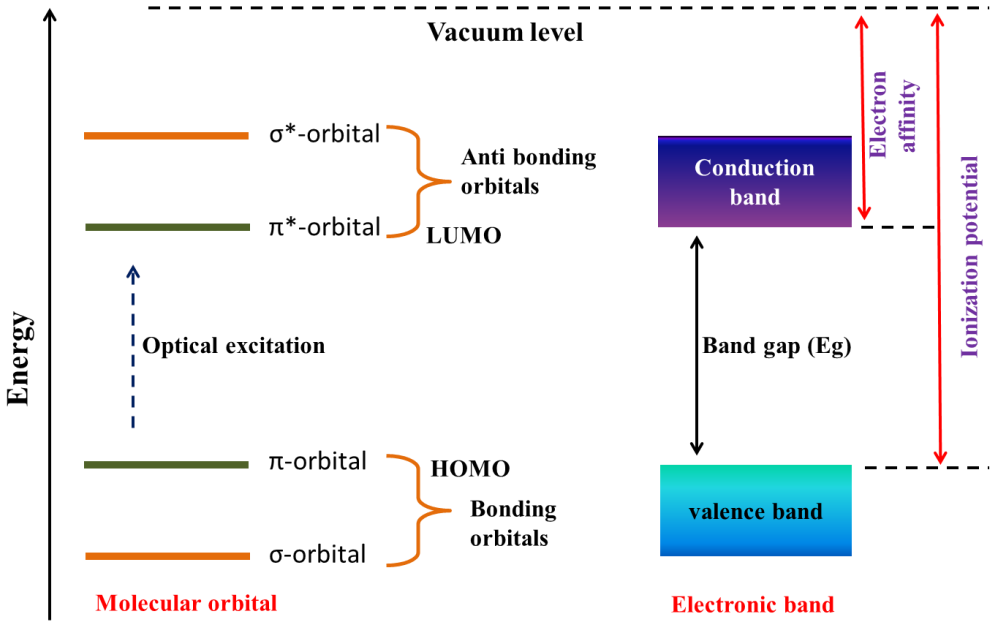

Figure 1.2: The comparative energy band diagram for conjugated polymer and conventional inorganic semiconductor.

The charge generation mechanisms in inorganic and organic photovoltaic devices are entirely different from each other due to the intrinsic electronic diversity between inorganic and organic materials that cause significant differences in the interfacial processes in inorganic and organic photovoltaic devices. The generation of free charge carriers in inorganic PV takes place directly upon light absorption under normal conditions. Whereas in the case of organic PV, the light absorption results in the production of a mobile excited state which dissociates into free charges only at the heterointerface where the tightly bonded (due to the Coulombic interaction) excitons are get dissociated by the driving force [16]. These generation phenomena affect the active material structure at the micro and nanoscopic scale, which is important for organic PV to be performed efficiently.

Another aspect of the inherently different electronic structure of inorganic and organic semiconductors is its charge transport phenomenon. In an inorganic semiconductor, typically band transport mechanism is observed where the surrounding lattice efficiently screens the delocalized charges due to the inorganic materials' high dielectric constant. Transportation of these delocalized charges takes place through the material in the continuous conduction band of the semiconductor without any energy losses, whereas, in amorphous organic semiconductors, the conductive electronic states are more localized. The dielectric constant is lower in organic semiconductors due to which charges are poorly screened by the neighboring molecules [17]. These poorly screened charges polarize and distort the surrounding lattice and form the polarons, which diffuse between adjacent molecules through a less efficient hoping mechanism, comparing to band transport, results in lower charge mobility in organic semiconductors as compare to that of inorganic semiconductors [15].

The entirely different cohesion forces in the amorphous organic solids and crystalline inorganic solids also explain these two materials' physical and mechanical properties. The inorganic semiconducting materials are rigid, highly brittle, and have very high processing temperatures, making them costly. On the other hand, organic semiconducting materials are semi-crystalline in nature, lightweight, flexible, and have very low processing temperature compared to inorganic semiconductors, which makes them cheaper materials for industrial processes [10]. The light absorption phenomenon in both semiconductors is different due to differences in their electronic structure. The absorption coefficient (α) ($\sim 10^5\ cm^{-1}$) of organic semiconductors in the visible range is higher when compared with the inorganic semiconductor ($\sim 10^3$ - $10^4\ cm^{-1}$). In general,

the bandgap of the conducting organic semiconductors lies between 1 eV- 2 eV, which is well suited for the visible spectrum to be absorbed [18].

Finally, the numbers of synthetically available inorganic semiconductors are much lower than that of their organic counterparts. Also, the electrical and optical properties of the organic semiconductors are effectively changed/tuned during the synthesis process by accurately designing the molecular structure and thus increasing the control on the performance optimization. All these advantages of organic PV over inorganic PV are well enough to develop the researchers' interest to work in the field of organic PV rather than the inorganic counterpart.

1.3.2 Type of Organic Photovoltaic Devices

Three types of structures, namely single-layer, bilayer heterojunction, and bulk heterojunction, are commonly used to fabricate organic photovoltaic cells. The brief introduction of these three types of photovoltaic devices is discussed in the following subsections.

1.3.2.1 Single-Layer OPV Device

A single photoactive film sandwiched between transparent and non-transparent electrodes with different work functions is used to fabricate a single-layer OPV device, as shown in Figure 1.3 (a). The first single-layer OPV was reported with very low quantum efficiency [19]. The low quantum efficiency was due to low charge mobility (μ) of organic semiconductor ($10^{-3}cm^2/V{\cdot}s$) in comparison with the inorganic semiconductor, i.e., single crystalline silicon ($10^{3}cm^2/V{\cdot}s$). The single-layer OPV device's power conversion efficiency was also very low (around 0.01%) due to the

lower charge mobility of organic photoactive semiconductor sandwiched between the charge extracting electrode [20].

In the single-layer OPV device, a Schottky barrier is formed between a low work function electrode and a semiconducting photoactive film (p-type semiconductor). The Schottky barrier creates a thin layer of depletion region that develops a built-in electric field. The developed built-in electric field facilitates the dissociation of generated excitons upon light absorption in such a way that generated excitons diffuse into the depletion region, and electrons are collected by the low work function electrode while holes are collected by high work function electrode, as shown in Figure 1.3 (b). The major concern with this type of structure is the low diffusion length of generated excitons. Therefore, most of the excitons are get recombined before dissociation and do not contribute to the photocurrent. Hence, the power conversion efficiency exhibited by the single-layer OPV devices is very low (0.01%) [20].

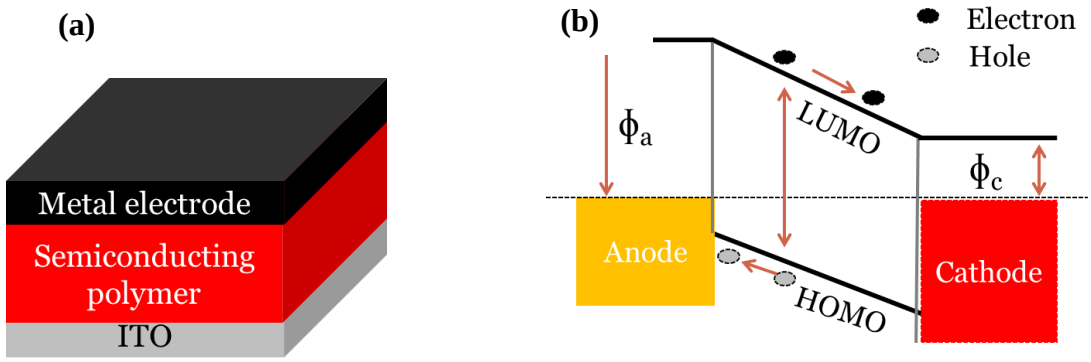

Figure 1.3: (a) Device structure and (b) Energy band diagram of single-layer OPV cell.

1.3.2.2 Bilayer Heterojunction OPV Device

To overcome the low-efficiency problem associated with the single-layer OPV device, a new device structure, i.e., donor/acceptor bilayer heterojunction, was

introduced by C. Tang in 1986 [13] with remarkable efficiency of 1%. The high-efficiency in bilayer OPV was made possible due to the pn junction formation using p-type and n-type organic semiconductor, generally called electron donor and electron acceptor material, respectively, as shown in Figure 1.4 (a). This bilayer of p-type and n-type semiconductor is worked as a photoactive layer. In particular, most of the time, the photogeneration of excitons takes place at the bilayer interface. The dissociation of the excitons occurs due to the presence of the built-in electric field at the junction (interface). The dissociation takes place in such a way that electrons are moved towards the acceptor by crossing the junction to the cathode and holes remain in the donor side and move towards the anode, as shown in Figure 1.4 (b). The probability of recombination of the electron-hole pairs is less as compared to that of single-layer OPV devices because this structure allows the excitons to cross the interface and separate in two different phases. However, the efficiency of the OPV devices is still low compared to the inorganic PV devices, mainly due to the low diffusion length of around few tens of nanometer and low interface area.

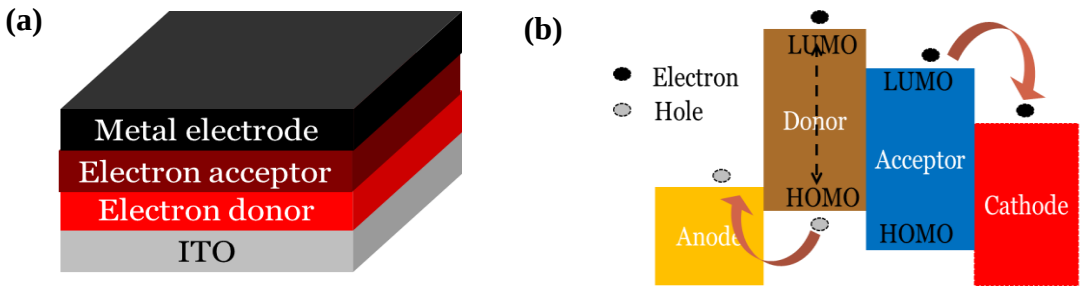

Figure 1.4: (a) Device structure and (b) Energy band diagram of bilayer heterojunction OPV device.

1.3.2.3 Bulk Heterojunction (BHJ) OPV Device

To further improve the efficiency of the OPV device new concept of bulk heterojunction was introduced where donor and acceptor semiconductors are blended to enhance the interface area so that generation of the electron-hole pair could be increased. The excitons generated near the interface can easily cross the junction to participate in the photogenerated current, rather than excitons generated far from the interface area. The BHJ OPV device and energy band diagram structures have been shown in Figure 1.5 (a) and (b), respectively. Significant improvement in efficiency has been obtained in BHJ OPV devices compared with the single-layer or bilayer OPV devices. Various p-type polymeric materials such as poly(p-phenylene-vinylene) (PPV), MEH-PPV, P3HT, PQT-12, PTB7-Th, PBDTTPD, MDMO-PPV and, PCDTBT etc., have been extensively used as a donor [21]–[26]. Whereas n-type fullerene derivatives such as C_{60}, C_{70}, $PC_{61}BM$, $PC_{71}BM$, etc., as well as some non-fullerene materials, have been used as an acceptor [27]. The higher efficiency in the BHJ OPV devices compared to bilayer OPV devices could be attributed mainly to the reduced exciton losses due to the large interfacial area and the reduced dimensions of donor and acceptor phase/ domains in which excitons are generated and diffuse to reach the donor/acceptor interface [28]. If the size or length of the donor/acceptor domain is comparable to that of the excitons diffusion length, then possibility of crossing the donor/acceptor interface by the excitons will be increased. this may lead to increase in photo-generated current and thereby increasing the efficiency of the BHJ OPV devices.

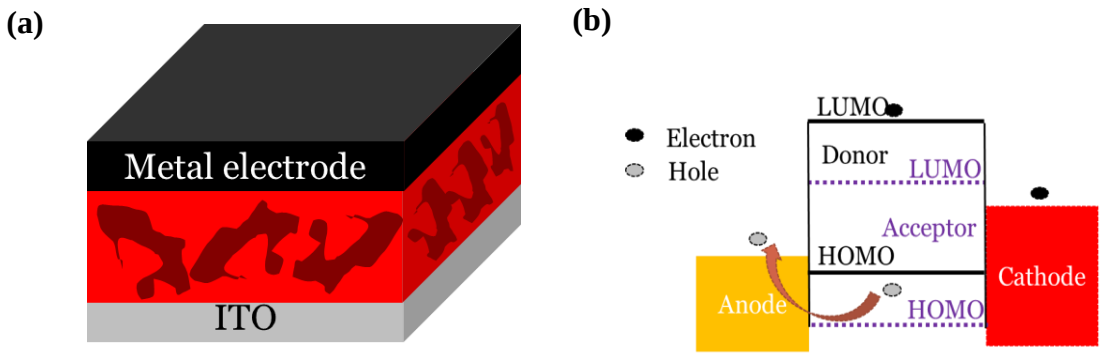

Figure 1.5: (a) Device structure and (b) Energy band diagram of bulk heterojunction (BHJ) OPV device.

The different device structures for the OPV are used for the improvement in the power conversion efficiency. Apart from the photoactive layer variation, buffer layers are also used to reduce recombination and improve OPV efficiency. The buffer layers are chosen in such a way that one type of charge carrier (i.e., electrons) can move one side, and another type of charge carrier (i.e., holes) can move another side so that no recombination can take place. These buffer layers are called the electron transport layer (ETL), and hole transport layer (HTL) as shown in Figure 1.6. ETL allows passing the electron through it and blocks the hole, whereas HTL allows the hole to pass through it and blocks the electrons. Sometimes interface layer (IL) is also used for better energy band alignment between the transport layer (ETL or HTL) and the photoactive layer. The suitable morphology of the different layers also plays a vital role in achieving high-efficiency BHJ OPV devices. Despite several difficulties in the performance improvements of BHJ OPVs, Zhu et al. [29] have recently reported a highly efficient BHJ OPV with the maximum efficiency ~ 16.88 %.

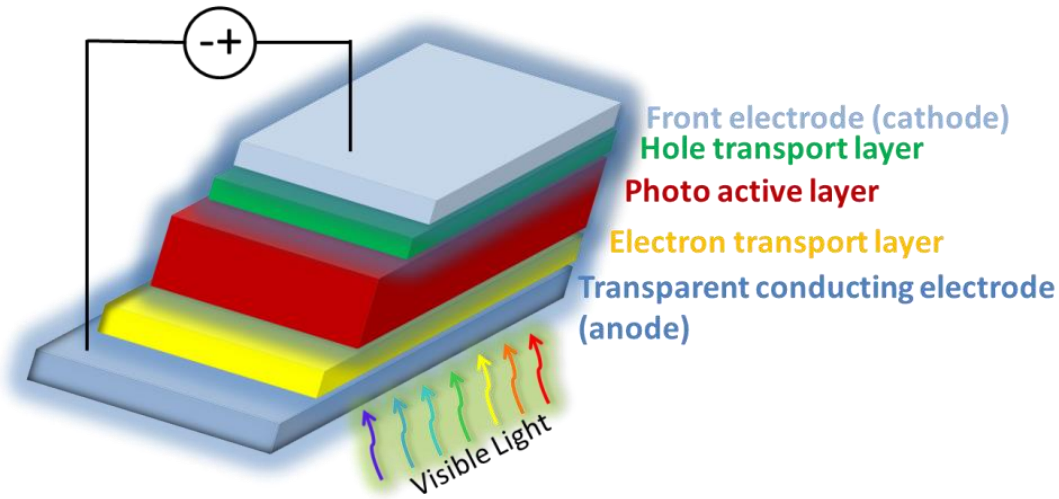

Figure 1.6: Bulk heterojunction (BHJ) OPV device with buffer layer.

1.3.3 Working Principles of BHJ OPV Device

To develop a better understanding of the performance of OPV devices, a comprehensive discussion on the working mechanism of the OPV devices is important. Therefore, for the deeper analysis, the working principle of OPV devices is discussed in this section. Figure 1.7 shows the basic working principle of OPV devices. Primarily, it consists of four basic steps that are (1) light absorption, (2) exciton diffusion, (3) Exciton dissociation, and (4) charge collection, as shown in Figure 1.7. In BHJ OPV devices, donor material absorbs most of the solar spectrum due to low bandgap (absorption coefficient of acceptor material is much lower and band gap is high). The following subsections describe the working principle of OPV devices in more detail.

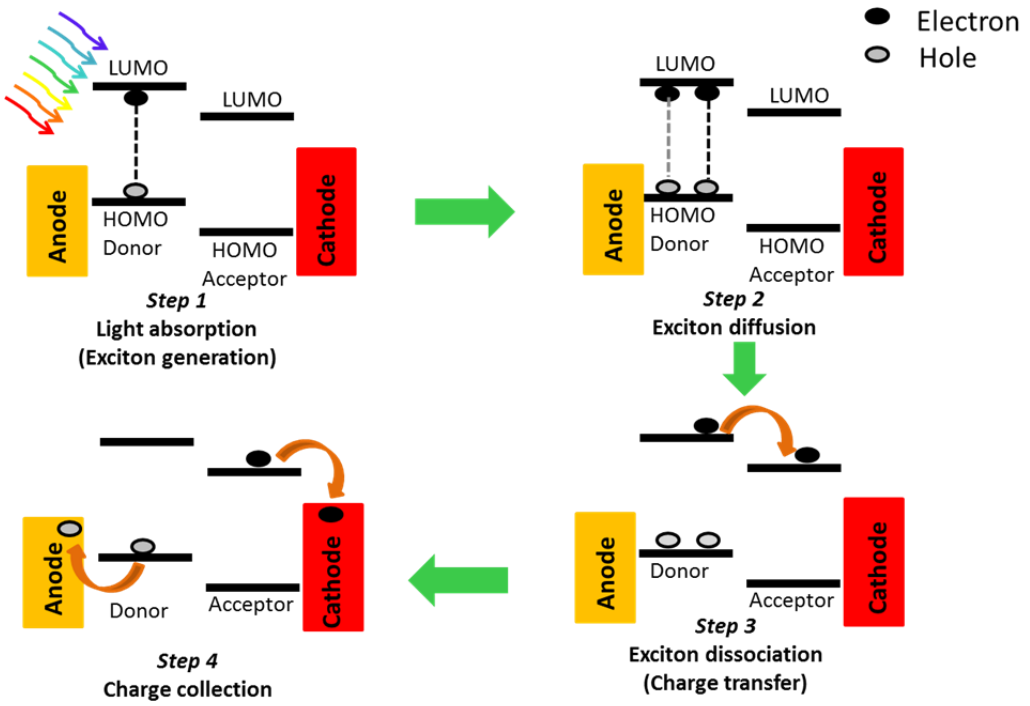

Figure 1.7: Working of BHJ OPV device: Step 1 to 4 [30].

1.3.3.1 Light Absorption

Light absorption is mainly due to the donor/acceptor blend (photoactive material), and within the donor/acceptor phase, absorption occurs mostly in the donor material. Penetration of the incident photons into the photoactive layer is taken place after illumination of the light on the device. The amount of light to be absorbed by the absorbing material depends primarily on the absorption coefficient of the donor and acceptor material. This absorption coefficient mainly depends on their molar extinction coefficient (i.e., the intrinsic capacity of light absorption by a single molecule), density, and absorption cross-section area. Moreover, light absorption also depends upon the bandgap (Eg) of semiconductors, defined by the difference between HOMO and LUMO. Only photons with energy > Eg could be absorbed. Therefore, the accurate tuning of the electronic structure of semiconductor molecular is required to maximize

light absorption. Another factor influencing light absorption is film thickness. As the absorption coefficient of organic semiconductor is much higher than that of the inorganic counterpart (Si), the thickness of organic semiconductor less than 100 nm is enough for 60% to 90% absorption of the incident light when reflective back contact is used [31].

Furthermore, the light pathway length inside the photoactive film also influences light absorption. The reflection, refraction, and scattering affect mostly this pathway length at the device layers interfaces and the device/air interface. Light absorption is also influenced by the format of the solar spectrum, which depend upon atmospheric condition. The emission of photons is distributed over the wavelength range of 2500 nm, and it is equivalent to the emission of a black body at 5960 K for the extra-terrestrial solar spectrum (AM0), as shown in Figure 1.8. However, this solar spectrum is filtered by the atmosphere when reached at the earth's surface, as shown in Figure 1.8. But the spectrum pattern remains the same, and it is called terrestrial solar spectrum (AM1.5), a standard for the calculation of PV parameters.

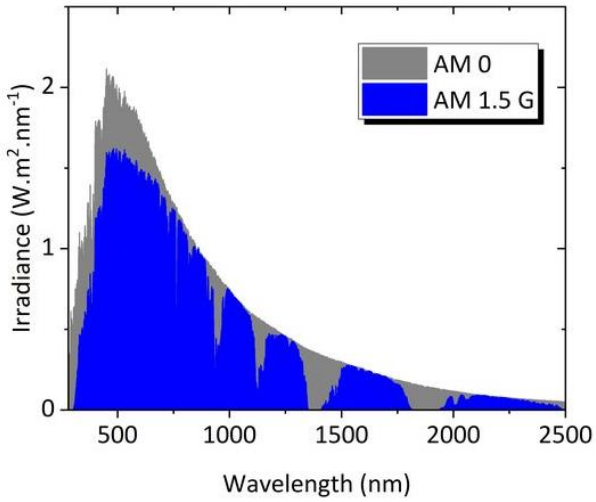

Figure 1.8: Extraterrestrial solar spectrum (AM0, gray) and terrestrial solar spectrum (AM1.5, blue) [32].

1.3.3.2 Exciton Diffusion

Once the solar light is absorbed in the donor material, the electrons are transferred from the ground state to one of the excited states of the semiconductor and results in a generation of excitons. The separation of these generated excitons can take place only when diffusion is allowed to the donor/acceptor interface. Diffusion is continued deeper till the recombination does not take place. The domain size of the donor material in the BHJ OPV device must be kept comparable to the exciton diffusion length so that the exciton recombination mechanism could not dominant and effective diffusion can take place. Typically, the exciton diffusion length of the donor phase in the BHJ OPV device ranging from 5 nm to more than 100 nm depending upon the donor material used [33].

1.3.3.3 Exciton Dissociation

After surviving the recombination process, the remaining excitons are diffused into the donor or acceptor phase and finally reached the donor/acceptor interface. Commonly, excitons dissociation has been described as a two-step process. In the first instance, at the donor/acceptor interface, the exciton state evolves into a charge transfer (CT) state between the donor (+ve) and acceptor (-ve). Then either recombine to the ground state or dissociates into free carriers via several charge-separated (CS) states (states where the electron and hole are weakly bounded with the Coulombic attraction force or freed from one another) [34]**.** The energy of the final CS state corresponds to the energy associated with the completely unbound electron-hole pair and related to the ionization potential of the donor (IP_D) and electron affinity of the acceptor (EA_A) (i.e $E_{final} = IP_D + EA_A$). The favorable condition for the excitons to be dissociated is when the difference between ionization potential of the donor (IP_D) and electron affinity of the

acceptor (EA_A) is greater than that of binding energy (E_B) of the excitons. The condition is as follow:

$$IP_D - EA_A > E_B \quad (1.1)$$

The rate of the charge transfer at the donor/acceptor interface is very efficient and fast, typically in the range of < 100 fs. Once the excitons are dissociated, the holes stay in the donor molecule itself, whereas electrons are moved towards the acceptor molecules. In this way, the charge carriers are spatially separated and reside in two different molecules that results in low recombination rates.

1.3.3.4 Charge Collection

The possible conditions for charge collection at their respective positive and negative electrodes are when the work function of the cathode is lower than the LUMO level of the acceptor material, and the work function of the anode is higher than the HOMO level of the donor material. Depending upon the difference between the work function of the electrodes and LUMO of the acceptor and HOMO of the donor, two types of contacts are formed, i.e., ohmic contact and non-ohmic contact. Non-ohmic contact causes electrical losses for the device, whereas ohmic contact facilitates better charge collection at their respective electrode, and higher efficiency could be expected. The most common electrodes used in the organic solar cell are silver (Ag), gold (Au), and aluminium (Al) as a non-transparent electrode and indium-doped tin oxide (ITO) and fluorine-doped tin oxide (FTO) as a transparent electrode [35]. ITO is a highly conducting semiconductor made up of SnO_2 (10%) and In_2O_3 (90%), and highly transparent for the visible light due to its high bandgap of approximately 3.7 eV and its high conductive is because of oxygen vacancies [36].

Charge extraction does not depend only on band alignment but also on various physical and chemical characteristics of the interface of electrode and semiconducting materials such as wave function hybridization, dipole formation, chemical reactions, and physical intermixing, etc. [37]. All these factors affect the mechanisms and efficiency of the charge extraction process at the interface of electrodes and semiconducting materials. For example, a thin oxide layer formed at the interface causes a potential barrier for charge extraction. On the other hand, while depositing the metal by using the evaporation method, the thermal energy of the metal causes hot metal atoms and clusters to diffuse into the semiconducting layer that creates non-geminate charge recombination sites and also results in damaging of the semiconducting layer due to high metal condensation energies. A buffer layer (ETL, HTL, IL) is used between the active and electrode layers to overcome these problems [38]. Commonly used HTLs are PEDOT:PSS (polymer) and some metal oxides such as vanadium oxide (V_2O_5), molybdenum oxide (MoO_3). On the other hand, primarily used ETLs are metal oxide of TiO_2 and ZnO.

1.3.4 Equivalent Circuit of BHJ OPV Devices

The structure and operation of BHJ OPV devices are similar to heterojunction diode; hence it is represented by the equivalent circuit using a simple diode connecting with a load resistance R_L when no light falls on it, as shown in Figure 1.9 (a). Upon the light illumination on the BHJ OPV device, a potential difference is developed when the terminals are open, and this developed voltage is called open-circuit voltage (Voc). On the other hand, a short circuit current (Isc) is drawn when terminals are connected. For any intermediate resistance R_L, a solar cell develops a voltage in the range of 0 to Voc and delivers a current I, such a way that $V = I*R_L$. The load resistance R_L connected to

the BHJ OPV device develops a potential difference between terminals even under dark condition. This potential difference is responsible for the diode current in the direction opposite to the photocurrent. The diode current is termed as dark current I_{dark}. Since most of the BHJ OPV device under dark condition behaves like a simple diode, the dark current is equal to diode current. It varies according to the diode behaviour shown by equation 1.2, known as Shockley's equation.

$$I_d = I_{so}\left[e^{\frac{V}{nV_T}} - 1\right] \tag{1.2}$$

Where, I_{so} is reverse saturation current, n is ideality factor of the diode, V_T thermal equivalent voltage and V is the voltage across the diode.

When light is illuminated on the solar cell, a photogenerated current I_{ph} occurs, and the total current will be denoted by equation 1.3.

$$I = I_{ph} - I_d \tag{1.3}$$

$$I = I_{ph} - I_{so}\left[e^{\frac{V}{nV_T}} - 1\right] \tag{1.4}$$

Some resistive elements, known as series resistance (Rs) and shunt resistance (Rsh), are also associated with practical OPV devices due to which the equivalent circuit of the solar cell gets modified, which includes Rs and Rsh [39], as shown in Figure 1.9 (b). Accordingly, equation 1.4 is modified to equation 1.5. For better performance of any solar cell, the value of series resistance must be as low as possible and Rsh must be as high as possible.

$$I = I_{ph} - I_{so}\left[e^{\left\{\frac{V-IRs}{nV_T}\right\}} - 1\right] - \frac{V-IRs}{Rsh} \tag{1.5}$$

Where, I_{ph} is photocurrent.

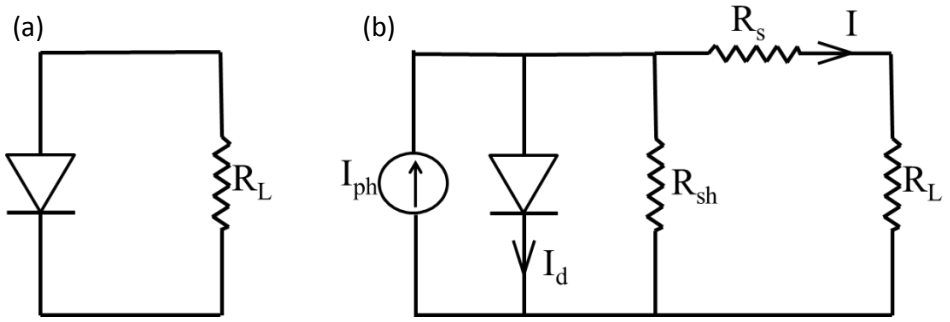

Figure 1.9: Equivalent circuit of OPV device under (a) Dark and (b) Solar light.

1.3.5 Parameters of BHJ OPV Devices

The BHJ OPV devices work as a simple diode under dark, and the current flowing through it follows the diode curve shown by the blue curve in Figure 1.10. When light falls on the BHJ OPV device, the current-voltage (I-V) curve follows the superposition of dark (I-V) and generated current upon illumination of light and gets sifted to the fourth coordinate, as shown in Figure 1.10 (red curve). All the important parameters of BHJ OPV devices, namely power conversion efficiency (η), short circuit current (Isc), open-circuit voltage (Voc), and fill factor (FF) are calculated directly from the solar cell current-voltage (I-V) characteristics, as shown in Figure 1.10. The parameters are briefly described in the following subsections.

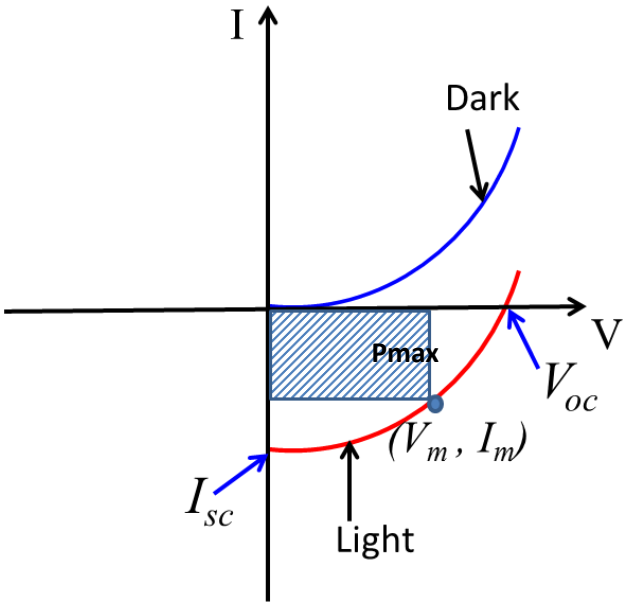

Figure 1.10: Current-voltage (I-V) characteristics of BHJ OPV.

1.3.5.1 Short Circuit Current (Isc)

A short circuit current is a current flowing through the cell when the voltage across the cell is zero (V=0), as shown in Figure 1.10**.** It is the maximum current that any BHJ OPV device can draw and deliver to the load against light illumination. The generation of short circuit current takes place due to the excitons generation and collection by the respective electrode. It can also be described as the total number of charge carriers generated and finally collected by their respective electrodes when there is no applied voltage. For any ideal BHJ OPV devices, the value of short circuit current (Isc) and photocurrent (Iph) must be equal. In general, the value of short circuit current depends on device area, and therefore most of the time, it is used as short circuit current density (Jsc in mA/cm^2) for the efficiency calculation purpose. Following are the factors upon which short circuit current depends on:

1. Directly proportional to the intensity of light falling on the device.
2. Electrical and optical properties of the photo absorber material.

3. Device area upon which light strikes and the overall spectrum of the incident light.
4. It also depends on the interface between the active layer and buffer layer through which the generated carriers have to be crossed.
5. Minority carrier lifetime. So that generated carriers can be collected by the electrode to convert in the current before recombination.

1.3.5.2 Open Circuit Voltage (Voc)

Open circuit voltage is one of the most important parameters to define the BHJ OPV devices' efficiency. It is the maximum voltage developed by the BHJ OPV device upon illumination of light when there is no external load connected, i.e., when the current flowing between the terminals is zero, as shown in Figure 1.10. Generally, the maximum limit of Voc depends on the energy offset between the HOMO of the donor material and LUMO of the acceptor material, as shown in Figure 1.11. Various factors that influenced the open-circuit voltage are shown in Figure 1.12. The most commonly used formula for calculating the open-circuit voltage (Voc) of the BHJ OPV device is described by equation 1.6 [40]. Where "e" is the electronic charge.

$$Voc = \frac{1}{e}[E_{LUMO}Acceptor - E_{HOMO}Donor] - 0.3 \quad (1.6)$$

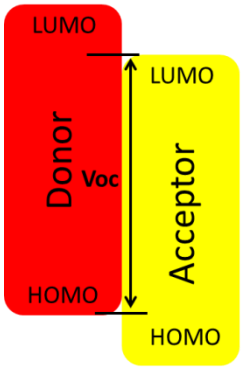

Figure 1.11: Maximum limit for open-circuit voltage in OPV.

Figure 1.12: Factors influencing the open-circuit voltage in OPV [40].

1.3.5.3 Fill Factor (FF)

The fill factor of any BHJ OPV device primarily gives an idea about the shape of the current-voltage (I-V) characteristic under light illumination condition. In other words, the fill factor defines the ideality of the BHJ OPV device. The maximum value of the fill factor could not be greater than one. It is defined as the ratio of the product of maximum voltage (Vm) and maximum current (Im) to the product of Voc and Isc. It is calculated by the formula described in equation 1.7. Graphically, it defined the

squareness of the current-voltage (I-V) characteristic of the BHJ OPV device and represented by the area under the shaded region, which also shows the region where the device delivers the maximum power to the load, as shown in Figure 1.10. The most important parameters that affect the fill factor are series resistance (Rs) and shunt resistance (Rsh) [41].

$$FF = \frac{V_m * I_m}{V_{oc} * I_{sc}} = \frac{P_{max}}{V_{oc} * I_{sc}} \quad (1.7)$$

1.3.5.4 Power Conversion Efficiency (PCE)(η)

Power conversion efficiency is the most discussed performance parameter of the BHJ OPV devices. This parameter shows the amount of light converted into electricity and is denoted by the ratio of output power to the input power, as shown by equation 1.8.

$$(PCE) = \frac{P_{out}}{P_{in}} = \frac{FF * V_{oc} * I_{sc}}{P_{in}} \quad (1.8)$$

Where Pin is input incident power falling on cell. The intensity of the sunlight changes depending upon the geographical location, so one standard is commonly maintained for the intensity of sunlight while calculating the power conversion efficiency of the solar cell. The standard test conditions are 25 C^o temperature, AM 1.5 spectral shape as standard air mass index, and 1000 W/m^2 intensity of light [42] for the calculation of power conversion efficiency. The most important factor that affects the power conversion efficiency is the fill factor. Suppose two cells have the same Voc and Isc but different fill factors, as shown in Figure 1.13. Despite having the same Voc and Isc the power conversion efficiency of cell 2 is higher than that of cell 1 due to a higher fill factor for cell 2 compared to cell 1.

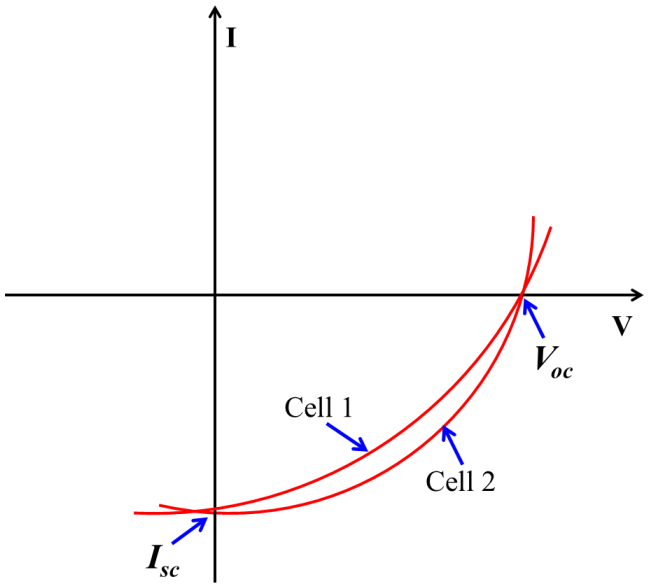

Figure 1.13: Comparison of power conversion efficiency of cell 1 and cell 2.

1.4 Literature Review

The present thesis primarily focuses on the effect of various layers on the performance parameters of the bulk heterojunction (BHJ) organic solar cell (OSC). To accomplish the motive of this thesis, we had already discussed the literature on inorganic-based photovoltaic devices to investigate the gap between inorganic and organic photovoltaics. Now, we have reviewed the literature based on organic photovoltaic to discuss the various aspects of the OPV device's performance depending on various layers associated with the BHJ OPV.

1.4.1 Review of BHJ OSCs

The organic solar cell using a single layer of small-molecule organic semiconductor deposited by the vacuum evaporation method was first reported by Calvin in 1958 [43]. Reucroft and Simpson investigated the photovoltaic effect in the monolayer of chlorophyll [44]. Merritt and Hovel fabricated an organic solar cell using a single-layer of hydroxy squarylium as an organic semiconducting dye in 1976 and achieved a power

conversion efficiency of only 0.2% [45]. Ghosh and Feng reported an organic solar cell based on Merocyanine-type photosensitizing dyes and achieved an efficiency of 0.7% in 1978 [46]. Later, a breakthrough occurred when Tang [13] gave the donor/acceptor bilayer-based organic polymer solar cell concept in 1986. He used the bilayer of copper phthalocyanine and perylene tetracarboxylic derivative for photoabsorption and reported the power conversion efficiency of 1%.

The small molecule blended junction was first reported by Hiramoto *et al.* in 1991 [47], [48]. They investigated the composite materials in the three-layer structure and achieved a maximum efficiency of 0.7%. MEH-PPV as a donor polymer and C_{60} as an acceptor polymer were used Sariciftci *et al.* and fabricated the bi-layer heterojunction photodiode as well as solar cell [49]. Whitlock *et al.* have investigated various materials and device structures for the organic solar cell [50]. In 1995, Yu, *et al.* [51] have given the concept of bulk heterojunction by using MEH-PPV donor and C_{60} acceptor and got the efficiency two times higher than that of the simple bilayer structure. Yang and Heeger have investigated the morphology of semiconducting polymer composites mixed with C_{60} used in the organic solar cell [52]. Chen *et al.* [53] have fabricated OPV using the multilayer of donor polymer MDMO-PPV and $PC_{61}BM$ as an acceptor polymer. They have also compared the performance of BHJ OPV to the single layer of MDMO-PPV. The relation between efficiency and morphology of donor-acceptor phase in BHJ OSC was investigated by Padinger *et al.* [54]. Fromherz *et al.* [55] have done a comparative study on the organic photovoltaic devices containing various blends of polymer and fullerene derivatives.

Chirvase *et al.* [21] have fabricated the OSC based on the P3HT donor and $PC_{61}BM$ acceptor and investigated the electrical and optical properties. Riedel and Dyakonov

have explored the charge transport in the P3HT:$PC_{61}BM$ based BHJ OSC [56]. Yuen *et al.* [57] have reported the comparative study of BHJ OSC based on PQT-12:$PC_{61}BM$ and P3HT: $PC_{61}BM$, and they found better stability in the case of OPV device fabricated with PQT-12: $PC_{61}BM$, but the power conversion efficiency was only ~0.45% rather than ~2.5% in case of device P3HT: $PC_{61}BM$. This report shows that PQT-12 could also be used as HTL or interface layer with another donor polymer to improve the stability as well as the efficiency of the BHJ OSC. From starting era to the current scenario of the OSC, several organic polymers have been explored to be utilized in the OSC [19], [21]–[23], [49], [58]–[60][24]. Beaupre and Leclerc have studied the performance of P3HT as well as PCDTBT based BHJ OSC separately and found that PCDTBT based BHJ OSC performed well [61]. Zhang *et al.* have performed the stability analysis of PCDTBT:$PC_{71}BM$ based BHJ OSC [26].

Apart from the organic semiconducting materials used as a photoactive layer, other layers such as transport layers (ETL and HTL) [62] [63] and interface [64] layer also play an important role in improving the performance parameters of the BHJ OSC. Metal oxides are extensively used material for the transport layer in BHJ OSC due to their better transparency in the visible region and good ohmic contact with the donor and acceptor polymers [65]–[69]. On the other hand, PEDOT:PSS is the most widely used organic polymer used as HTL in BHJ OSC [63], [70]. One of the earliest works on the solution-processed ZnO ETL layer in P3HT: $PC_{61}BM$ based OSC was carried out by White *et al.* in 2006 [71]. They achieved the certified power conversion efficiency of 2.58% by inserting solution-processed ZnO between ITO and active layer P3HT: $PC_{61}BM$. Hori *et al.* [72] have fabricated the C60/poly(3-hexylthiophene)(PAT6) based OSC where they used ZnO and MoO_3 as ETL and HTL layer, respectively.

Comparatively, they improved efficiency from 0.49% to 1.46% when ZnO and MoO_3 transport layers were inserted as ETL and HTL layers, respectively. Kundu *et al.* [73] have fabricated and characterized two different devices with structure, i.e., ITO/ZnO/P3HT: $PC_{61}BM$ /MoO_3/Ag and ITO/MoO_3 /P3HT: $PC_{61}BM$ /ZnO/Ag where solution-processed ZnO has been used as an ETL and thermally evaporated MoO_3 as an HTL layer. They found the efficiency enhancement from 2.86% to 3.48% when ITO/ZnO/P3HT: $PC_{61}BM$ /MoO_3/Ag device structure is used rather than ITO/MoO_3 /P3HT: $PC_{61}BM$ /ZnO/Ag device structure.

1.4.2 Review of PCDTBT: PCBM based BHJ OSCs

Semiconducting polymer have shown the great interest in the field of BHJ OSC in the recent year [22], [23], [58], [59], [74], [75]. Among various semiconducting polymer, poly[N-9′-hep- tadecanyl-2,7-carbazole-alt-5,5-(4′,7′-di-2-thienyl-2′,1′,3′-benzothiadiazole)] (PCDTBT) has shown great impact in BHJ OSC due to its superior properties over other semiconducting polymer [58], [61], [76]–[79]. Blouin *et al.* [58] have reported the highly conjugated and stable poly(N-alkyl-2,7-carbazole) derivative, namely poly[N-9′-hep- tadecanyl-2,7-carbazole-alt-5,5-(4′,7′-di-2-thienyl-2′,1′,3′-benzothiadiazole)] (PCDTBT) for the BHJ OSC. They have achieved a maximum efficiency of 3.6% in the PCDTBT: $PC_{61}BM$ based organic solar cell. They have also studied stability improvement using PCDTBT instead of mostly used donor polymer P3HT. Chu *et al.* [80] have reported the PCDTBT:$PC_{61}BM$ based BHJ OSC and examined the effect of PCDTBT:$PC_{61}BM$ thickness to improve the light absorption and hence increase the performance of the device.

Investigation on the effect of solvent on the morphology, charge transportation, and performance of PCDTBT:$PC_{70}BM$ based BHJ OSC have been carried out by Alem *et al.* [76]. Etzold *et al.* [79] have studied the charge dissociation and recombination phenomenon in PCDTBT:$PC_{61}BM$ based BHJ OSC. Effect of the nanostructured morphology of the PCDTBT:$PC_{70}BM$ film in the BHJ OSC has been reported by Sun Moon et al. [78]. Ratcliff *et al.* [81] have discussed the influence of energy level alignment between the buffer layer and the PCDTBT:$PC_{70}BM$ active layer in the BHJ OSC. Parlak *et al.* [58] have synthesized the Ag nanoparticle and utilized the same in PCDTBT:$PC_{61}BM$ based BHJ OSC for the comparative study of the performance of the two distinct devices fabricated with and without Ag nanoparticle.

Researchers have introduced several approaches to improve the performance of PCDTBT:$PC_{61}BM$ based BHJ OSC in the recent year [61], [77], [84]–[88]. Further, one of the most critical investigation of the stability of the PCDTBT:$PC_{71}BM$ based BHJ OSC has been carried out by Zhang *et al.* [26] recently in 2016. They have fabricated and characterized the PCDTBT:$PC_{71}BM$ based BHJ OSC and reported the outdoor stability analysis of one year. Tuning of PCDTBT:$PC_{71}BM$ and nanoparticles blend have been performed by D'Olieslaeger *et al.* [89] for the eco-friendly solution processing of polymer solar cell. Pratyusha *et al.* [90] have fabricated PCDTBT:$PC_{70}BM$ based BHJ OSC incorporating the ternary polymer made of PCDTBT, $PC_{70}BM$, and PCPDTBT to enhance the absorption range and reported the improved performance of the device.

Furthermore, the analysis of traps' effect due to the disorder assembly of the donor-acceptor phase on the charge transport between donor and acceptor polymer in PCDTBT:$PC_{70}BM$ based BHJ OSC has been reported by Khan *et al.* [91]. Aghassi and

Fay have reported the effect of the isopropyl alcohol (IPA) treatment on the performance of the PCDTBT:$PC_{70}BM$ and (p-DTS($FBTTh_2$)$_2$: $PC_{70}BM$ based BHJ OSC [92]. Recently in 2020, Piralaee *et al.* [83] have analysed the effect of random dispersion of Ag nanoparticles in the P3HT:$PC_{61}BM$ and PCDTBT:$PC_{61}BM$ photoactive blends. They found the enhancement in the photocurrent and thus the improved performance of the BHJ OSC.

1.4.3 Major Observation from the Literature Review

In this section, we will summarise the major observations derived from the literature survey, as given in the following:

- The donor/acceptor polymer-based bulk heterojunction type organic solar cells [47], [48] have shown great interest in the field of OPV due to its several advantages such as low cost and easy fabrication processing technique, flexibility, and the possibility of enhancement in the power conversion efficiency by utilizing the various approaches [83], [91], [92].
- Among various donor polymers, the polymer poly[N-9′-hep- tadecanyl-2,7-carbazole-alt-5,5-(4′,7′-di-2-thienyl-2′,1′,3′-ben- zothiadiazole)] (PCDTBT) [58], [61], [76]–[79] has been reported as a better candidate to replace the most widely used donor polymer poly(3-hexylthiophene) (P3HT) due to its higher stability and performance when blended with the fullerene derivative $PC_{61}BM$ (electron acceptor) in BHJ OSC [80].
- Among the various metal oxides, used as a transport layer in the BHJ OSC, ZnO and MoO_3 is the most promising candidate for the ETL and HTL, respectively due to its high transparency in the visible region [65]. Whereas

PEDOT:PSS [63] is extensively used as organic HTL in BHJ OSC due to its high transparency and easy solution processability.

- PQT-12 is used as a donor polymer and shows higher stability than extensively used donor polymer P3HT [57]. Although PQT-12 offers lower power conversion efficiency than P3HT, it may also be used as HTL as well as interface layer in the BHJ OSC due to its higher stability and higher mobility than P3HT [24].
- It has been observed from the literature that inverted structure (transparent electrode/ETL/active layer/HTL/metallic electrode) of the BHJ OSC is more stable than the conventional structure (transparent electrode/HTL/active layer/ETL/metallic electrode) of the BHJ OSC [73].

1.5 Challenges in the BHJ OSC

It has been discussed that the BHJ OSCs, where organic polymers are used as photo absorbing material, are gaining more popularity due to their various advantages, namely low cost, easy fabrication process, the possibility of flexible, roll to roll fabrication (large area fabrication) process, and non-toxicity (due to organic material). However, BHJ OSCs are facing several challenges in achieving high efficiency as well as stability. Further, due to the use of several layers, they also face the challenge of achieving a better interface between the different layers, leading to lower charge transportation and lower performance. Many approaches have been employed to improve the performance of BHJ OSC, such as using an interface layer between the transport layers and active layer (PCDTBT:$PC_{61}BM$), optimizing the thicknesses of various layers, and incorporation third material in the active layer to improve the charge transportation.

1.6 Motivation and Problem Definition

In the previous section, we have already discussed the challenges related to the BHJ OSC, which includes the stability issue, lower efficiency, and low charge transportation due to the degradation issue of active layer material as well as the inappropriate interface between the various layers. Because of the relatively high performance of the PCDTBT donor polymer over the extensively used donor polymer P3HT in BHJ OSC, the PCDTBT polymer is believed to have a vast opportunity to improve the performance of the BHJ OSC when used with the different buffer layers. In the continuation of the above discussion, a highly stable PCDTBT donor polymer and $PC_{61}BM$ acceptor polymer are used for fabricating the BHJ OSC and characterize the performance parameters when used with the various buffer configuration layers. In addition, PQT-12 is used as HTL as well as interface layer deposited by floating film transfer method (FTM) to achieve better phase matching. Further, CdSe QDs are also used with the active layer (PCDTBT:$PC_{61}BM$) to enhance the BHJ OSC performance.

1.7 Scope of the Thesis

The present thesis deals with the fabrication and characterization of PCDTBT:$PC_{61}BM$ based BHJ OSC. The thesis consists of FIVE chapters, including the present chapter. The contents of the remaining FOUR chapters are briefly described in the following sentences:

Chapter-2 deals with the fabrication and characterization of PCDTBT:$PC_{61}BM$ based BHJ OSC, where FTM deposited PQT-12 polymer is used as interface layer in between active layer (PCDTBT:$PC_{61}BM$) and hole transport layer (PEDOT:PSS). The entire device is fabricated on the ITO-coated glass substrate. Here, PQT-12 provides

better band alignment and phase matching for the efficient charge extraction at their respective electrodes. The effect of PQT-12 interface layer on the device has been primarily carried out by electrical and optical characterization. The incorporation of the PQT-12 interface layer in PCDTBT:$PC_{61}BM$ based BHJ OSC improves performance and stability.

Chapter-3 includes the fabrication and characterization of PCDTBT:$PC_{61}BM$ based BHJ OSC device in ITO/ZnO QDs/ PCDTBT:$PC_{61}BM$/PQT-12/Ag structure, where ZnO QDs, PCDTBT:$PC_{61}BM$, and PQT-12 are used as ETL, active, and HTL layer, respectively. Several devices have been fabricated with different thicknesses of ZnO QDs and PQT-12 to optimize thicknesses of the individual layers for achieving the high-performance OPV device. Electrical and optical characterizations have been carried out to compare different fabricated devices. Among the various set of fabricated devices, it has been found that the BHJ OSC device with the thickness of 35 nm, 100 nm, and 20 nm for ZnO QDs, active and PQT-12 layer, respectively, provide the best performance.

Chapter-4 investigates the fabrication and characterization of PCDTBT:$PC_{61}BM$ based binary and ternary BHJ OSC. CdSe QDs are mixed with the PCDTBT:$PC_{61}BM$, and the complete device is fabricated on the ITO coated glass substrate in ITO/ZnO QDs/ PCDTBT:$PC_{61}BM$:CdSe QDs/MoO_3/Ag structure. All the layers are deposited by spin coating technique except MoO_3 and Ag, which are deposited by the thermal evaporation method. The comparative studies have been carried out for two different BHJ OSC devices fabricated without CdSe QDs and with CdSe QDs. CdSe QDs incorporated ternary BHJ OSC device has shown the superior solar cell performance compared to without CdSe QDs based binary BHJ OSC.

Finally, **Chapter-5** summarizes the major objectives and concludes the important findings of the present thesis. This chapter also outlines some future scope of works related to this thesis.